# Resonance parameters of the vector charmonium-like state G(3900)

[PRD 112 (2025), 016015]



Quanxing Ye,<sup>1</sup> Zhenyu Zhang,<sup>1</sup> Meng-Lin Du,<sup>2\*</sup> Ulf-G. Meißner,<sup>3†</sup> Peng-Yu Niu,<sup>1‡</sup> and Qian Wang<sup>1§</sup>

\*du.ml@uestc.edu.cn †meissner@hiskp.uni-bonn.de ‡niupy@m.scnu.edu.cn §qianwang@m.scnu.edu.cn

<sup>1</sup>South China Normal University, Guangzhou, China

<sup>2</sup>University of Electronic Science and Technology of China, Chengdu, China

<sup>3</sup>Universität Bonn, Bonn, Germany

#### 1. Abstract

Motivated by the updated analysis of the G(3900) by the BESIII collaboration, we perform a global analysis of the cross sections of the  $e^+e^- \to D\bar{D}, \ e^+e^- \to D\bar{D}^* + c.c., \ e^+e^- \to D^*\bar{D}^*$  processes, especially focusing on the properties of the G(3900). As the energy region of interest is limited by the next opening threshold, i.e. the  $D_1\bar{D}$  threshold, we focus on the energy region [3.7, 4.25] GeV, where three charmonia  $\psi(1D), \psi(3S)$  and  $\psi(2D)$  explicitly contribute to the cross sections. By constructing the P-wave contact interaction between the  $(D, D^*)$  doublet and its antiparticle in the heavy quark limit, we extract the physical scattering amplitude by solving the Lippmann-Schwinger equation. No matter whether three or two charmonium states are included in our framework, we always find a dynamically generated state corresponding to the G(3900), which suggests it to be a P-wave dynamically generated state. We also predict several dynamically generated states in the corresponding  $1^{-+}$  channel. These states can be further searched for in the electron-positron annihilation process involving the emission of a single photon.

#### 2.1 Formalism

•Convention: The hadronic basis can be written as  $|D^{(*)}\bar{D}^{(*)}\rangle_n^a$ , with a=d,u,s denoting the light quarks in the charmed meson pairs  $(cq)(\bar{c}\bar{q})$  and n=1,2,3,4 representing different charmed meson pairs  $D\bar{D}, D\bar{D}^*$ ,  $D^*\bar{D}_{S=0}^*$  and  $D^*\bar{D}_{S=2}^*$ . The SU(3) flavor basis can be written as  $|D^{(*)}\bar{D}^{(*)}\rangle_n^i$ , where the index i=0,8,1represents SU(3) singlet 0, the zero components of octet  $8^{00}$  and isospin triplet  $1^{10}$ , in order, where the superscripts denote the isospin I and its third component, respectively.

• The transformation from SU(3) flavor basis to the hadronic basis can be written as:

$$[|D^{(*)+}D^{(*)-}\rangle^d, |D^{(*)0}\bar{D}^{(*)0}\rangle^u, |D_s^{(*)+}D_s^{(*)-}\rangle^s]^T$$

$$= R[|D^{(*)}\bar{D}^{(*)}\rangle^0, |D^{(*)}\bar{D}^{(*)}\rangle^8, |D^{(*)}\bar{D}^{(*)}\rangle^1]^T,$$
(1)

where the transformation matrix R is

$$R = \begin{pmatrix} \frac{1}{\sqrt{3}} & \frac{1}{\sqrt{6}} & \frac{1}{\sqrt{2}} \\ \frac{1}{\sqrt{3}} & \frac{1}{\sqrt{6}} & \frac{-1}{\sqrt{2}} \\ \frac{1}{\sqrt{3}} & \frac{-2}{\sqrt{6}} & 0 \end{pmatrix} \otimes 1_{4\times4}, \tag{2}$$

• Based on the transformation, we can construct the contact potentials with respect to the Heavy Quark Spin Symmetry (HQSS):

$$V_{nn'}^{i} = {}_{n}^{i} \langle (D^{(*)}\bar{D}^{(*)}) | \mathcal{H}_{CT} | D^{(*)}\bar{D}^{(*)} \rangle_{n'}^{j} \delta_{ij},$$
(3)

where  $|D^{(*)}\bar{D}^{(*)}\rangle_n^j$ , have been decomposed into heavy-light basis. The potential of the bare state and open charmed meson pair reads as:

$$V_{c\bar{c}\ nj}^0 = {}_{n}^0 \langle D^{(*)}\bar{D}^{(*)}|\mathcal{H}_{\text{bare}}|j\rangle^0, \tag{4}$$

where j = 1, 2, 3 (j = 1, 2) denote charmonia  $\psi(1D)$ ,  $\psi(3S)$ ,  $\psi(2D)$  for Model I  $(\psi(1D), \psi(3S))$  for Model II). The schematic diagram of the interactions is shown in Fig. 1.

• With these contact potentials, we can solve the Lippmann-Schwinger equation (LSE) to obtain the T-matrix of open charm channels

$$T_{\text{oo}}(E) = \left[ \left[ \hat{V}_{\text{oo}}^{\text{eff}}(E) \right]^{-1} - G_{CT}(E) \right]^{-1}, \tag{5}$$

where the effective potential is defined as  $\hat{V}_{\text{oo}}^{\text{eff}} \equiv V_{\text{oo}} + V_{\text{ob}} G_{c\bar{c}} V_{\text{bo}}$ . Similarly, the production amplitudes is written as:

$$\mathcal{U}_{o}(E) = (1_{12 \times 12} - \hat{V}_{oo}^{eff} G_{CT}(E))^{-1} \hat{F}_{o}^{eff},$$
(6)

with  $\hat{F}_{o}^{\text{eff}} \equiv F_{o} + V_{ob}G_{c\bar{c}}f_{b}$  the effective bare production amplitude. The schematic diagram of the T-matrix and the physical production amplitude is shown in Fig. 2.

• We deduce the cross sections formula for the direct comparison with the experimental data:

$$\frac{d\sigma_n^a}{d\cos\theta} = \frac{|p_{D^{(*)a}}|}{16\pi s^{3/2}} |\overline{\mathcal{M}_n^a}|^2, \tag{7}$$

where  $|\mathcal{M}_n^a|^2$  is the square of the scattering amplitude. The production amplitude  $\mathcal{U}_0$  is a part of  $|\mathcal{M}_n^a|^2$ .

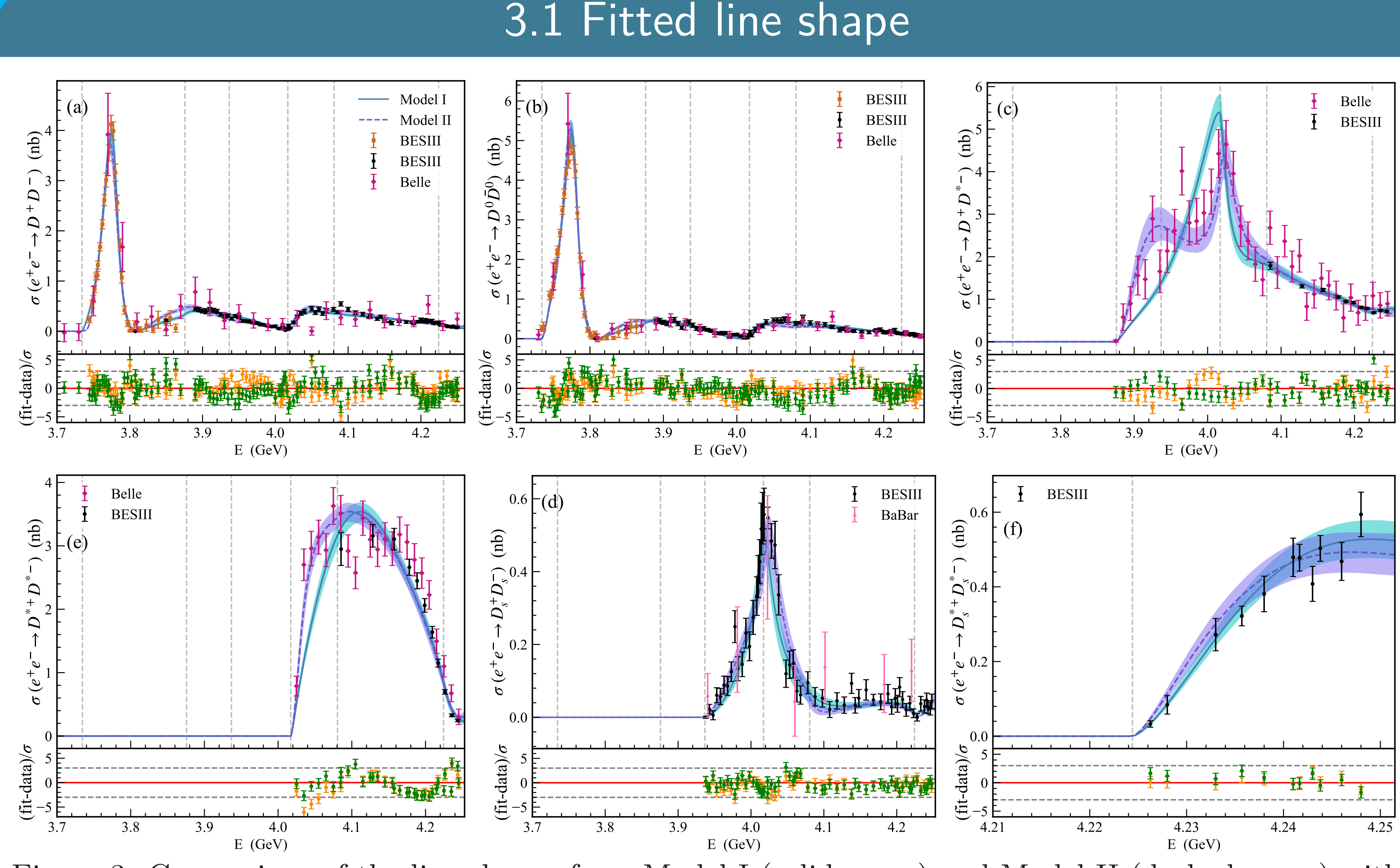


Figure 3: Comparison of the line shapes from Model I (solid curve) and Model II (dashed curve) with the experimental data. The blue and purple bands indicate the 99% confidence levels of Model I and Model II, respectively. The lower panels show the standardized residuals, where the orange and green points correspond to Model I and Model II.

## 3.4 Conclusion

We perform a global fit to the  $e^+e^- \to D^{(*)}\bar{D}^{(*)}$  processes in Fig. 3. With the fitted parameters presented in Tab. 1, we extract the pole positions presented in Tab. 2. The trajectories of poles in Tab. 2 are presented in Fig. 4.

### (1) Model I case

•From Fig. 4, it can be seen that the 3691.60 MeV,  $3778.42 \pm 11.81i$  MeV and  $4232.78 \pm 23.96i$  MeV ploes correspond to the  $\psi(2D)$ ,  $\psi(1D)$  and  $\psi(3S)$  vector charmonia. The pole  $4011.05 \pm 10.13i$  MeV is considered as a dynamically generated state.

• Another dynamically generated state is found at  $3832.57^{+0.91}_{-0.79} \pm 74.53^{+0.68}_{-2.15}i$  MeV on (-, +, -, +, +, +) sheet. After testing, it significantly impacts the physical region. The imaginary part of the pole causes a broad distribution, allowin a non-negligible probability for the state to lie above the  $[DD^*]_{Thr}$ . Thus, it can still decay to  $DD^*$ , making it a possible G(3900) candidate.

### (2) Model II case

• By performing a pole trajectory analysis similar to Model I, the poles  $3775.29 \pm 14.31i$  MeV and  $4278.21 \pm 21.59i$ MeV correspond to the  $\psi(1D)$  and  $\psi(3S)$  charmonia, respectively, while the other poles are considered as dynamically generated states. The pole at  $3883.91^{+0.38}_{-0.46} \pm 46.53^{+1.22}_{-1.22}i$  MeV on the (-, -, +, +, +, +) sheet is 9 MeV above the  $[D\bar{D}^*]_{Thr}$  threshold and can be considered as a candidate of the G(3900).

• Fig. 5 presents a comparison of the G(3900) pole position with results from other works.

- 4. Summary
- A coupled channel analysis of the  $e^+e^- \to D^{(*)}\bar{D}^{(*)}$  processes in HQSS and SU(3) within the energy region [3.7,4.25] GeV. • Pole position of G(3900):  $3832.57^{+0.91}_{-0.79} \pm 74.53^{+0.68}_{-2.15}i$  MeV for Model I and  $3883.91^{+0.38}_{-0.46} \pm$
- $46.53^{+1.22}_{-1.22}i$  MeV for Model II. • G(3900) is a dynamically generated state, instead of a renormalized charmonium.
- Predict several dynamically generated states in the  $J^{PC} = 1^{-+}$  channel.

#### 2.2 Interaction

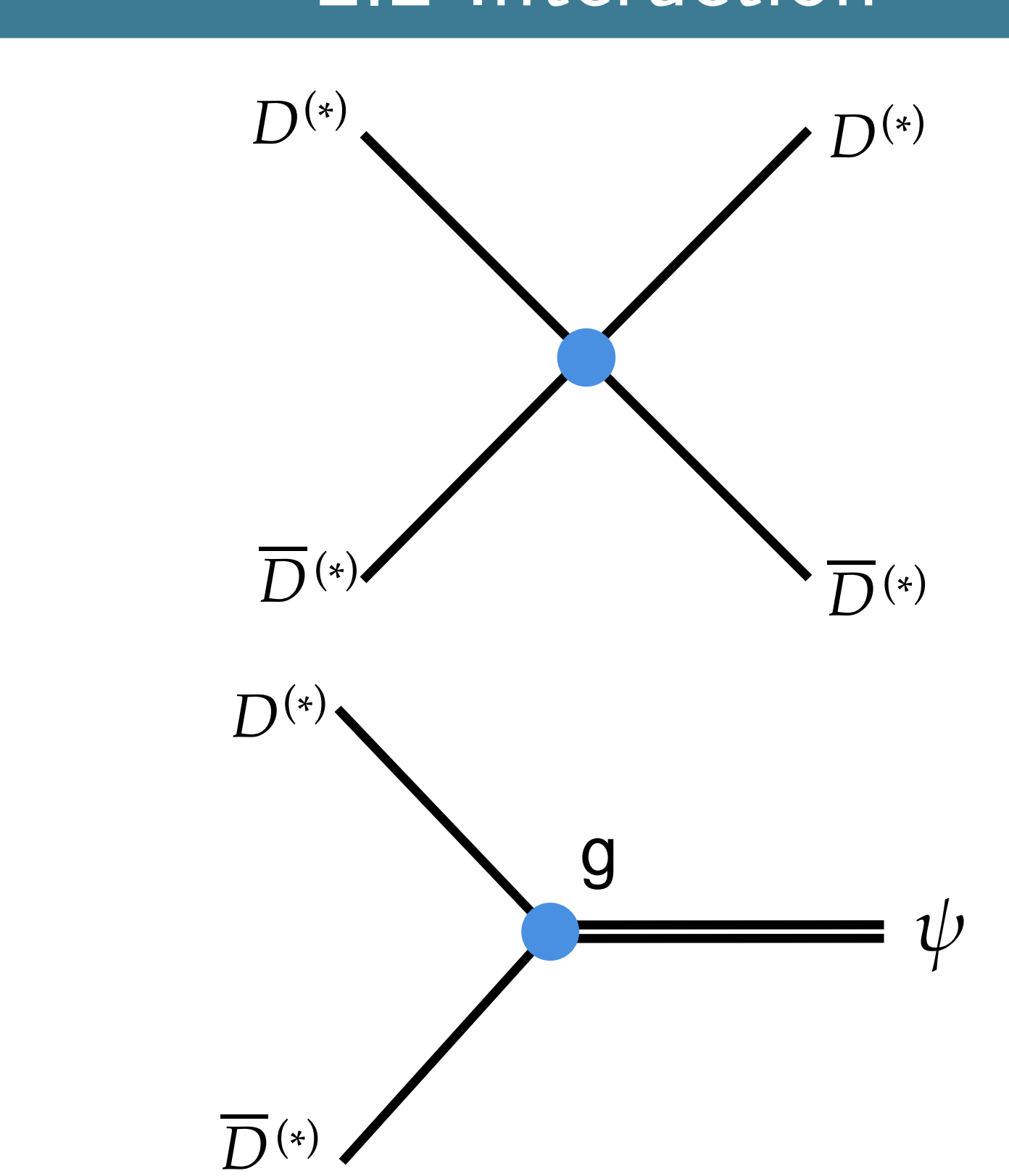


Figure 1: Schematic diagram of the interactions between charm-meson pairs and between charm-meson pairs and charmonia.

### 2.3 Re-summation

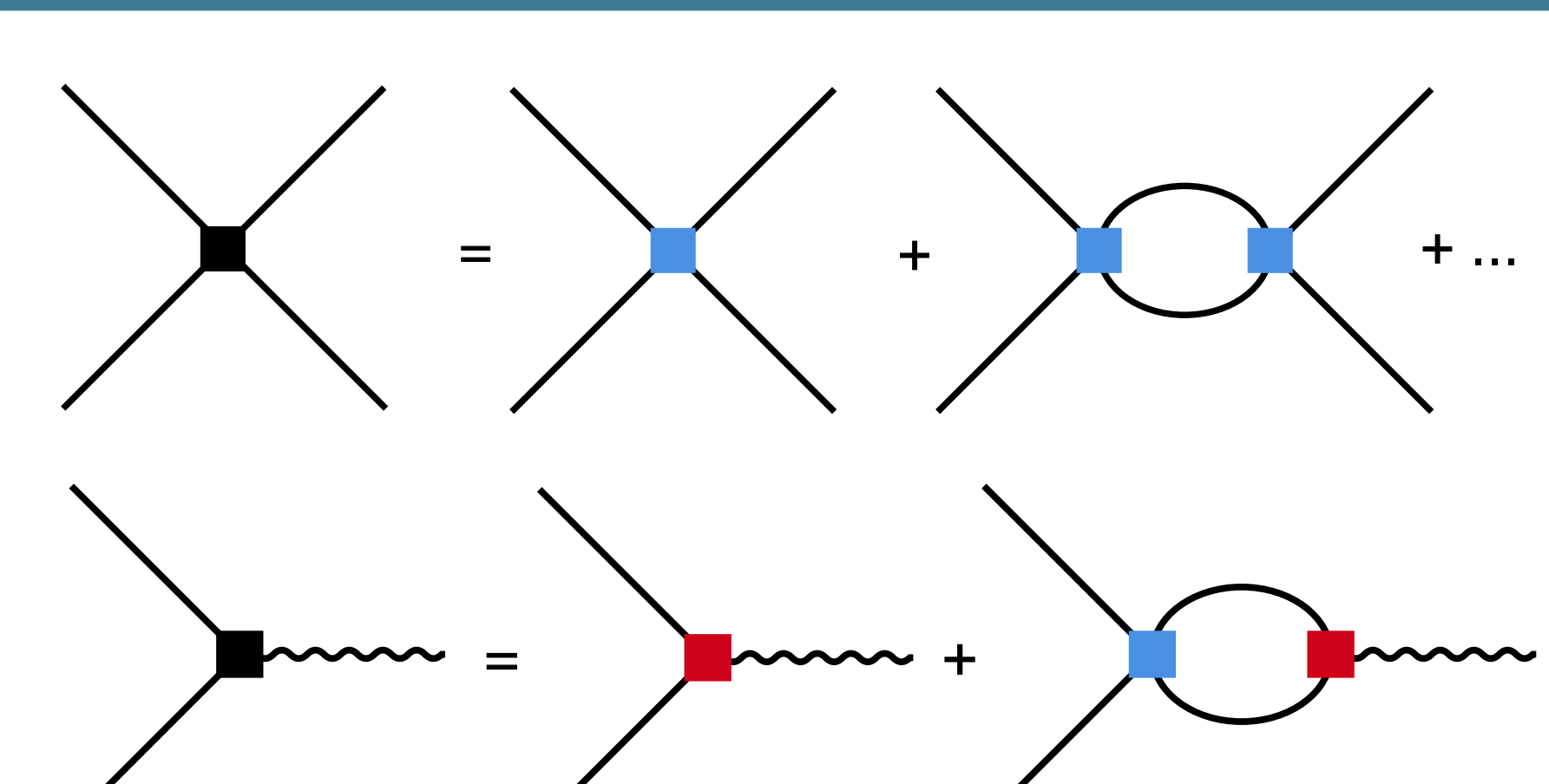
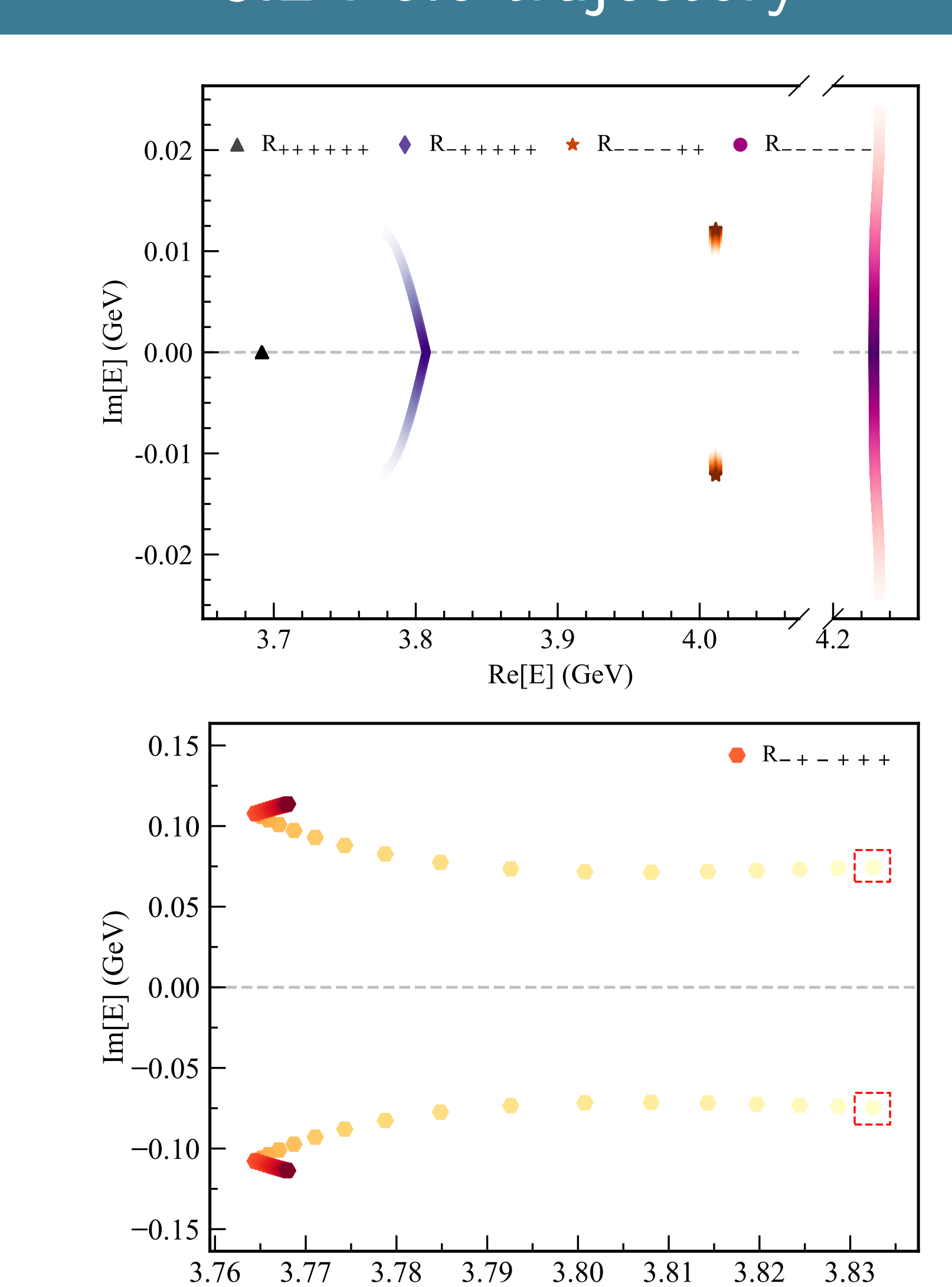


Figure 2: Schematic diagram of the T-matrix and

the physical production amplitude.

## 3.2 Pole trajectory



Re[E] (GeV) Figure 4: Upper panel: Trajectories of the poles in Model I on various Riemann sheets (RSs). Lower panel: Trajectory of pole  $3832.57^{+0.91}_{-0.79} \pm 74.53^{+0.68}_{-2.15}i$ MeV on the (-, +, -, +, +, +) Riemann sheet (RS).

# 3.3 Parameter and pole position

Parameters	Model I	Model II
$g_{1D}^{0} [\text{GeV}^{-1}]$	$0.66 \pm 0.04$	$-12.93 \pm 0.26$
$g_{3S}^{0} [\text{GeV}^{-1}]$	$-14.66 \pm 0.37$	$-14.11 \pm 0.96$
$g_{2D}^{0} [\text{GeV}^{-1}]$	$-17.09 \pm 0.23$	_
$m_{1D}^{\overline{0}}$ [GeV]	$3.807 \pm 0.001$	$3.804 \pm 0.001$
$m_{3S}^{\bar{0}}$ [GeV]	$4.229 \pm 0.002$	$4.253 \pm 0.005$
$m_{2D}^{00}$ [GeV]	$3.692 \pm 0.003$	_
$\Lambda \ [{ m GeV}]$	$0.50 \pm 0.00$	$0.50 \pm 0.00$
$\sqrt{2}/d$ of	9.17	2.66

Table 1: Part of fitted parameters.  $g_{1D}^0, g_{3S}^0, g_{2D}^0$ denote the bare couplings between the charmonia  $\psi(1D), \ \psi(3S), \ \psi(2D)$  and open charmed meson pairs.  $m_{1D}^0$ ,  $m_{3S}^0$ ,  $m_{2D}^0$  represent the bare mass of  $\psi(1D)$ ,  $\psi(3S)$ ,  $\psi(2D)$ .

	$\mathbf{RSs}$	Model I	Model II
	(+, +, +, +, +, +)	3.691.60	_
		_	$3743.07 \pm 7.36i$ [7]
(-	(-, +, +, +, +, +)	$3778.42 \pm 11.81i$ [12]	$3775.29 \pm 14.31i$ [14]
	(-,+,-,+,+,+)	$3832.52 \pm 74.53i$	_
	(-, -, +, +, +, +)	_	$3883.91 \pm 46.53i$ [47]
	(-,-,-,-,+,+)	$4011.05 \pm 10.13i$ [16]	$4019.42 \pm 17.40i$ [17]
	(-,-,-,-,-)	$4232.78 \pm 23.96i$ [24]	$4278.21 \pm 21.59i$ [22]

Table 2: Pole positions on the various RSs close to the physical one. The numbers in square brackets represent energy distances of the poles to the physical RS, in units of MeV.

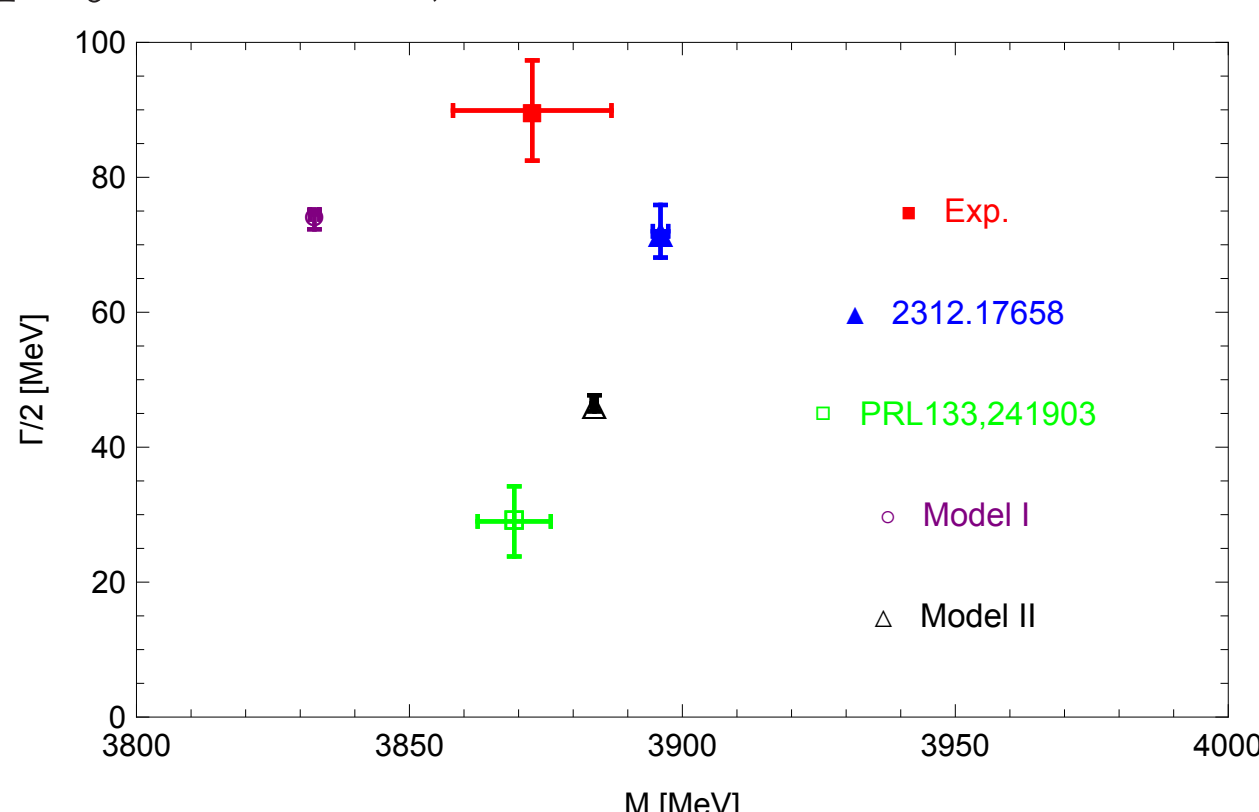


Figure 5: The pole positions of Model I (purple hollow circle) and Model II (black hollow triangle) in comparison with other works.